

PY5021 - 5 Sensor Types (2)

J. M. D. Coey

School of Physics and CRANN, Trinity College Dublin

Ireland.

1. Superconducting sensors
2. Resonance sensors
3. Optical sensors



Comments and corrections please: jcoey@tcd.ie

www.tcd.ie/Physics/Magnetism

Sensor	Principle	Detects	Frequency	Field (T)	Noise	Comments
Coil	Faraday's law	$d\Phi/dt$	$10^{-3} - 10^9$	$10^{-10} - 10^2$	100 nT	bulky ,absolute
Fluxgate	saturation	H	dc - 10^3	$10^{-10} - 10^{-3}$	10 pT	bulky
Hall probe	Lorentz f'ce	B	dc - 10^5	$10^{-5} - 10$	100 nT	thin film
MR	Lorentz f'ce	B^2	dc - 10^5	$10^{-2} - 10$	10 nT	thin film
AMR	spin-orbit int	H	dc - 10^7	$10^{-9} - 10^{-3}$	10 nT	thin film
GMR	spin accum.n	H	dc - 10^9	$10^{-9} - 10^{-3}$	10 nT	thin film
TMR	tunelling	H	dc - 10^9	$10^{-9} - 10^{-3}$	1 nT	thin film
GMI	permability	H	dc - 10^4	$10^{-9} - 10^{-2}$		wire
MO	Kerr/Faraday	M	dc - 10^5	$10^{-9} - 10^2$	1 pT	bulky
SQUID It	flux quanta	Φ	dc - 10^9	$10^{-15} - 10^{-2}$	1 fT	cryogenic
SQUID ht	flux quanta	Φ	dc - 10^4	$10^{-15} - 10^{-2}$	30 fT	cryogenic
NMR	resonance	B	dc - 10^3	$10^{-10} - 10$	1 nT	Very precise

Sensor Types (2)

4.4. Superconducting sensors

Flux quantization. dc and ac SQUID design. Flux-locked loops. Flux transformer design, dynamic response, slew rate. Comparison of low and high T_C SQUIDS. Signal/noise in SQUIDS. Mixed sensors. Noise reduction in SQUIDS.

4.5 Resonance sensors

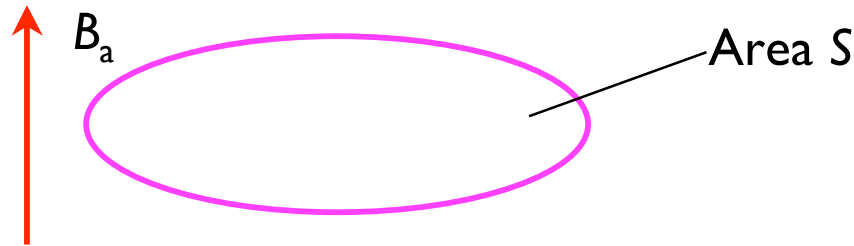
Nuclear precession. Proton magnetometer, Optical pumping, Cs and Rb magnetometers. Miniaturization, Illustration of integrated resonance sensors. Ultimate sensitivity and precision

4.6 Optical sensors

Faraday effect. Optical fibres. Field and rotation sensors.

4.4 Superconducting sensors

An important property of a resistanceless circuit is that **the flux threading a resistanceless circuit cannot change**



Cool the ring below its superconducting transition in a field B_a , applied in the normal state. The flux threading the loop is

$$\Phi = B_a S$$

Now try to change the flux in the ring by changing B_a .

An emf is induced according to Faraday's law. $\mathcal{E} = -S dB_a/dt$ and a current i is created.

$$S dB_a/dt = -Ri - Ldi/dt$$

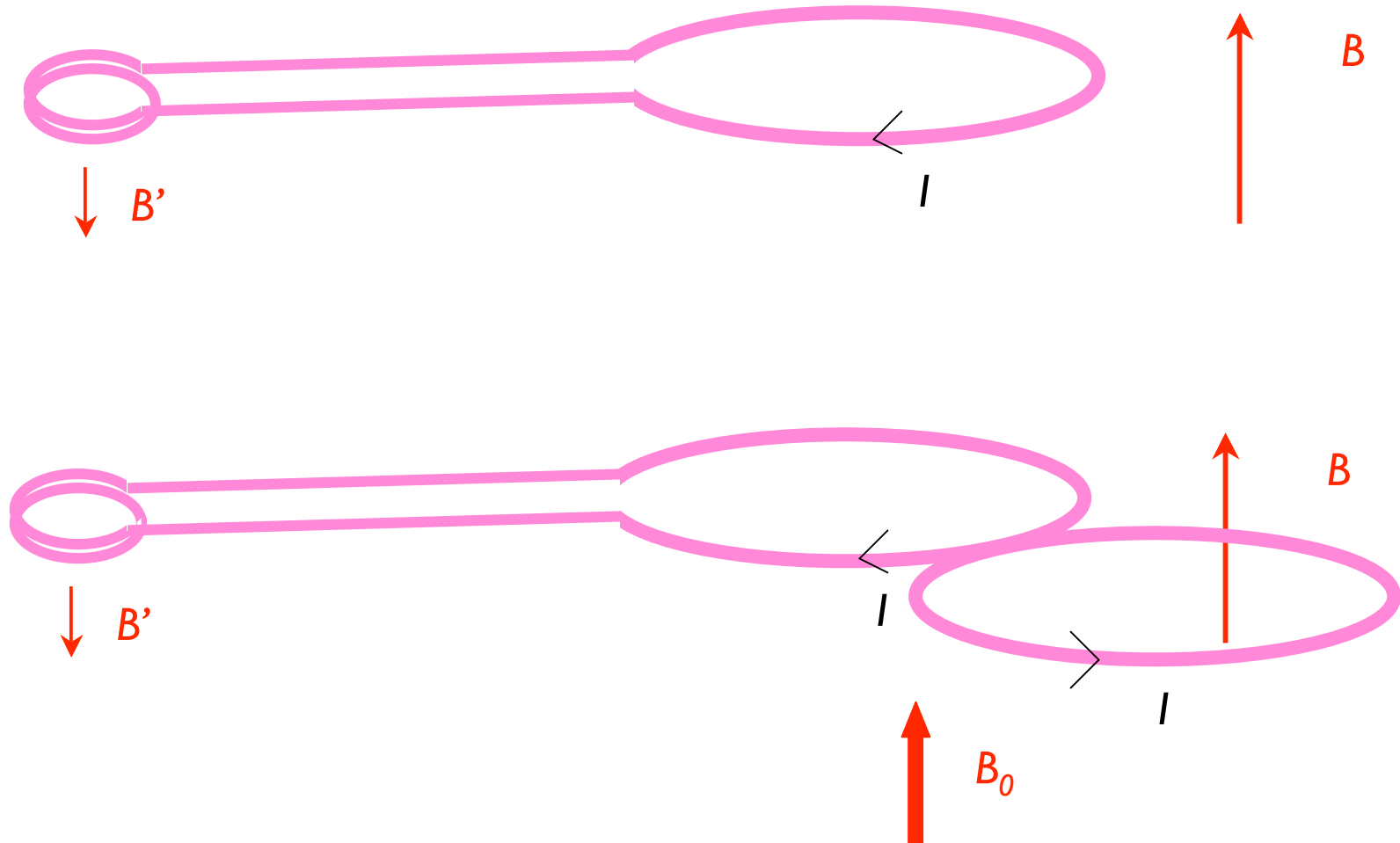
$$\text{Therefore constant} = Li + SB_a = \Phi$$

The total flux threading the circuit is a constant. It cannot change. The original flux is maintained indefinitely, provided the ring remains resistanceless, and $i < i_c$

- Uses:**
- Magnetic screening
 - Flux transformers
 - Superconducting magnets in the persistent mode.

Flux transformer.

A superconducting circuit. The flux threading the loop cannot change.



The *gradiometer* has a figure-of-8 pickup coil, which eliminates the effect of any uniform (fluctuating) field B_0 and responds to the local field B

4.4.1 Flux Quantization

There is a wavefunction of the form

$$\psi = \psi_0 \exp i\theta$$

which describes the superconducting electrons, where θ is the phase, a *macroscopic* variable. There is no supercurrent when $\theta(\mathbf{r}) = \text{constant}$.

Well inside a superconductor, the wave function ψ will give a uniform density of superconducting electrons.

$$|\psi|^2 = |\psi_0|^2 = n_s$$

Consider a loop carrying a supercurrent \mathbf{j} .

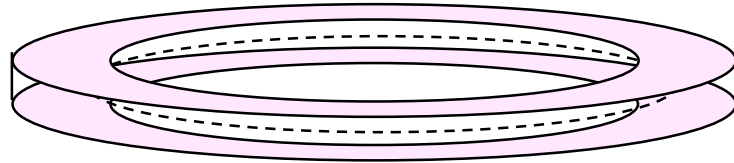
$$\mathbf{v} = (1/m)(\mathbf{p} - q\mathbf{A}) = (1/m)(-i\hbar\nabla - q\mathbf{A})$$

$$\therefore \text{The particle flux is } (1/2m)\{\psi^*(-i\hbar\nabla - q\mathbf{A})\psi + [(-i\hbar\nabla - q\mathbf{A})\psi]^*\psi\}$$

$$\therefore \text{Hence the current density is } \mathbf{j} = (1/2m)\{q(\psi^*\mathbf{v}\psi) + \text{cc}\}$$

$$\mathbf{j} = (n_s q/m)\{i\hbar\nabla\theta - q\mathbf{A}\} \quad (1)$$

A dramatic consequence of (I) is flux quantization in a superconducting ring



Consider the dashed line buried deep inside the superconductor, where $\mathbf{B} = \mathbf{j} = 0$

$$\oint \mathbf{j} \cdot d\mathbf{l} = (n_s q/m) \int \{i\hbar \nabla \theta - q\mathbf{A}\} \cdot d\mathbf{l} = 0$$

By Stokes's theorem, $\oint \mathbf{A} \cdot d\mathbf{l} = \int_S \nabla \times \mathbf{A} \cdot d\mathbf{S} = \int_S \mathbf{B} \cdot d\mathbf{S} = \Phi$

Φ is the enclosed flux, which is independent of path, provided we avoid the penetration depth.

Also $\oint \nabla \theta \cdot d\mathbf{l} = \Delta \theta$, the change of phase on going once around the ring.

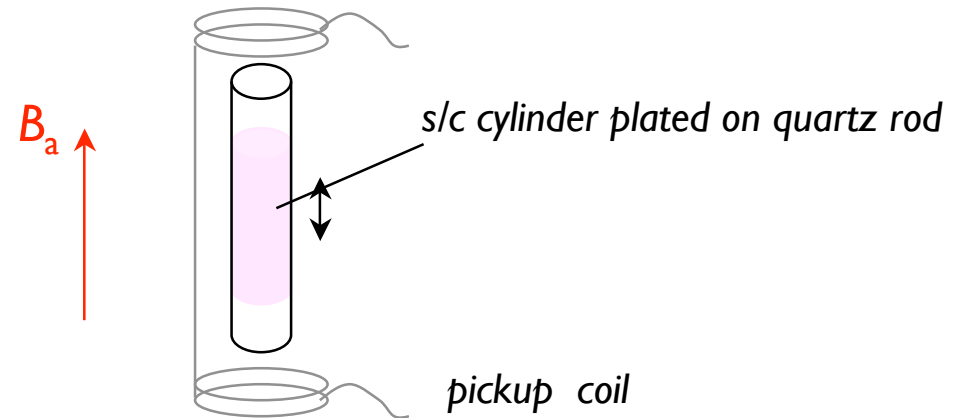
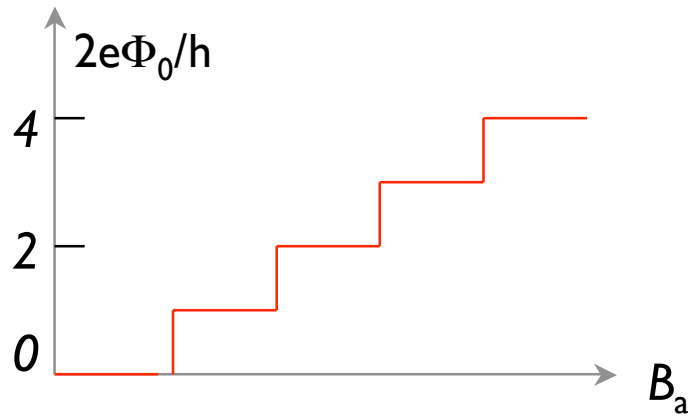
But ψ has to be single-valued, hence $\Delta \theta = 2n\pi$ or $\hbar \Delta \theta = \hbar 2n\pi$

$$\hbar 2n\pi - q \Phi = 0$$

$\Phi = \hbar 2n\pi/q = nh/q$ The flux is a multiple of a fundamental quantum h/q

$$\Phi_0 = 2.07 \cdot 10^{-15} \text{ T m}^2 \text{ the flux quantum or } \textit{fluxon}$$

Measurement of the flux quantum:



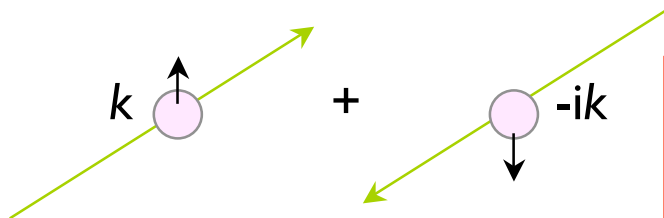
The fact that the flux quantum is actually observed is good evidence for the description of superconductivity in terms of the complex order parameter

$$\psi(\mathbf{r}) = \exp i\theta(\mathbf{r}).$$

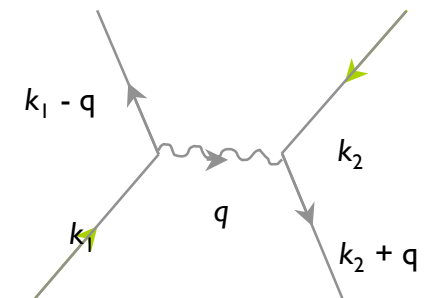
Furthermore, the charge q must be $2e$, not e , in order to explain the value of Φ_0 .

This means that the charge carriers are electron pairs. These are the Cooper pairs.

When no current flows, the pairs have no net momentum, $\theta(\mathbf{r})$ is constant.

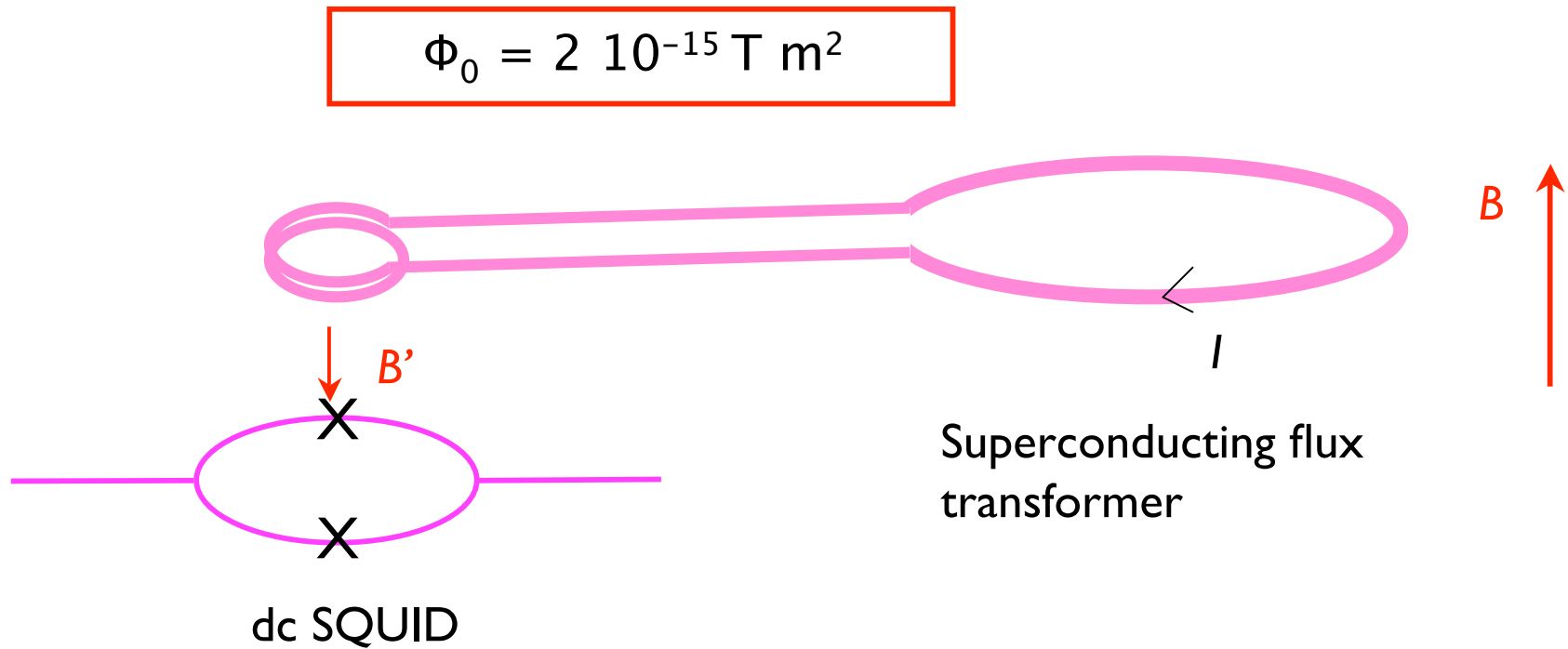


Cooper pair:	$q = 2e$	$m = 2m_e$
	$K = 0$	$S = 0$



4.4.2 Superconducting quantum interference devices.

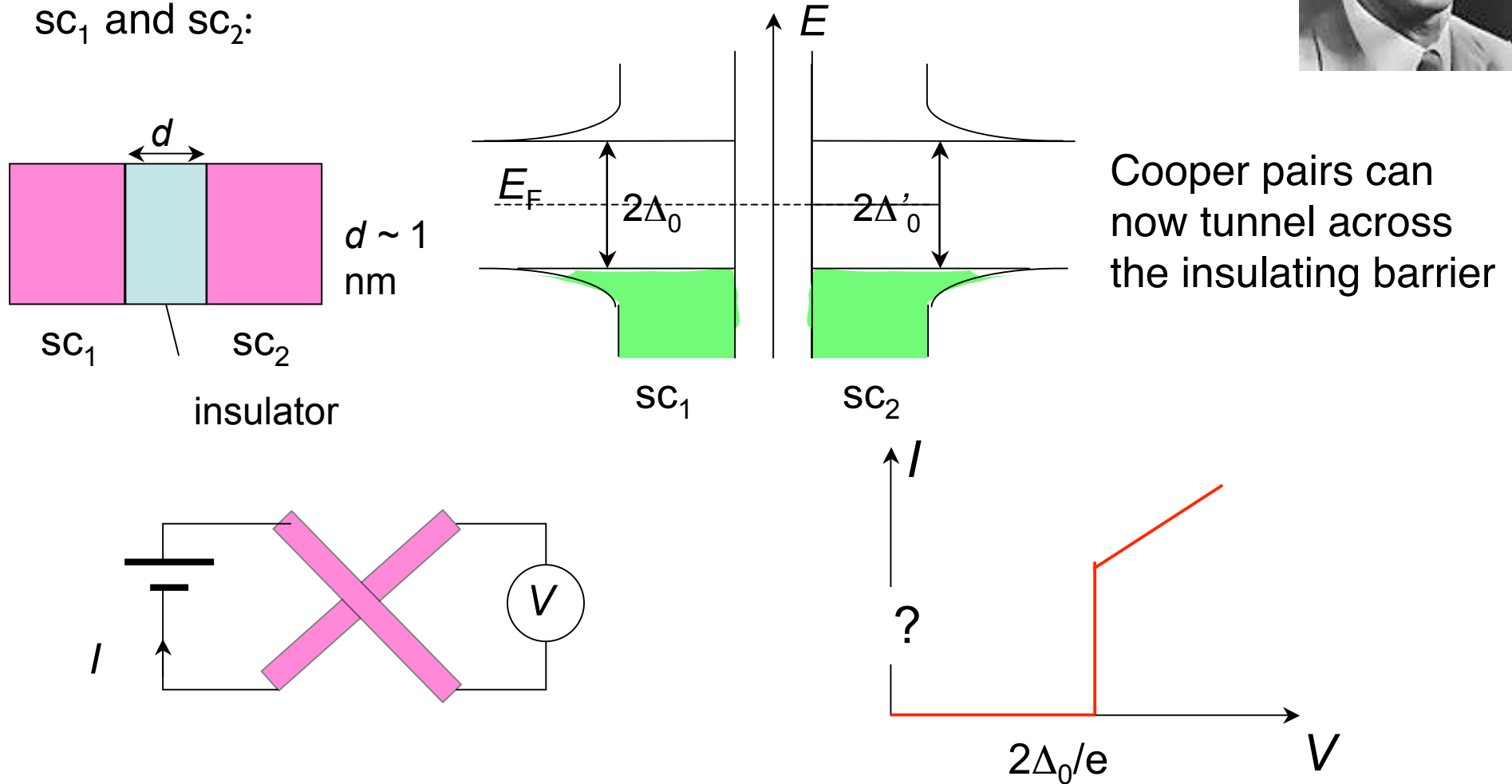
SQUIDs detect the change of flux threading a flux-locked loop. The flux is generally coupled to the SQUID via a superconducting flux transformer. The device is sensitive to a small fraction of a flux quantum. SQUIDS offer ultimate field sensitivity. They generally operate with a flux-locked loop.



Josephson tunneling.



(PhD work of Brian Josephson in 1963 — Nobel Prize 1973)
Consider a tunnel junction made from two superconductors sc_1 and sc_2 :



The two superconductors are weakly coupled across the insulating barrier.
Does a supercurrent flow?

Suppose the two superconductors are made of the same material, so $\Delta_0 = \Delta_0'$. The density of superconducting electrons n_s is the same in both, so they are described by a wavefunction with the same amplitude ψ_0 . What may be different is the phase θ .

$$\psi = \psi_0 \exp i \theta$$

If a supercurrent is crossing the junction, in zero applied field

$$j = (1/2m)\{q (\psi^* \mathbf{v} \psi) + cc\} \quad (\text{section 3.5})$$

Set $q = 2e$, $m = 2m_e$

$$j = -(eh/me)n_s \nabla \theta$$

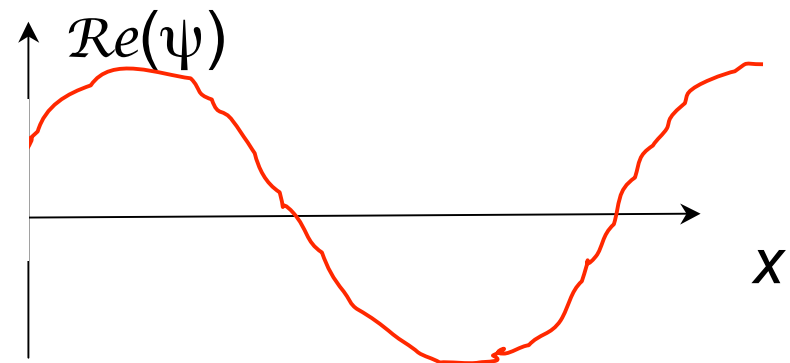
If $\nabla \theta = 0$, there is no current, and $\theta = \text{const.}$ If $j \neq 0$, $\nabla \theta \neq 0$

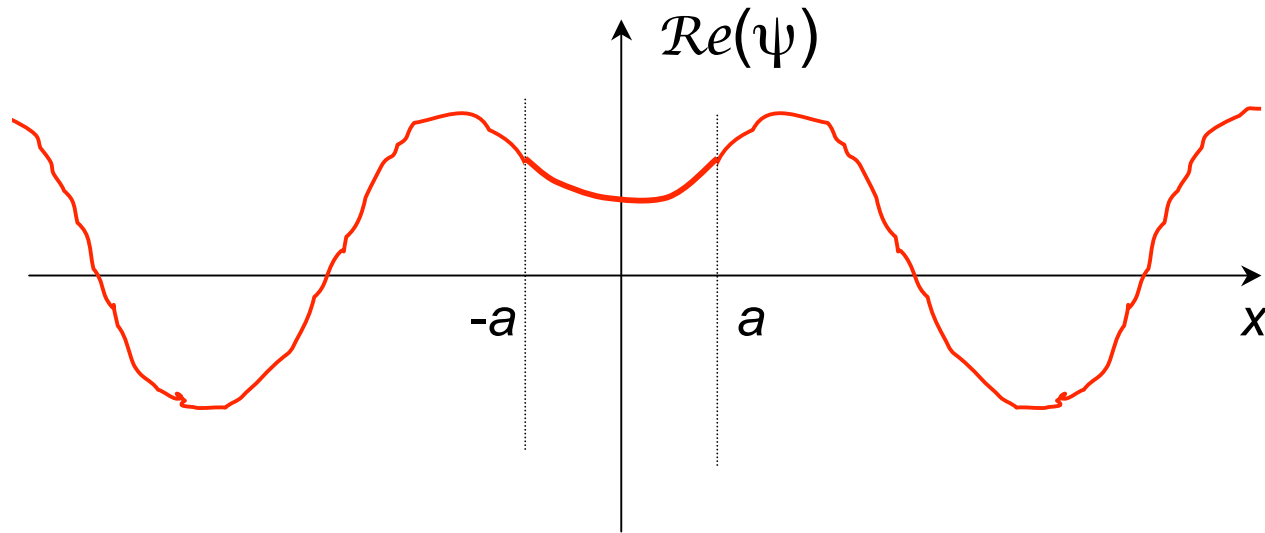
When a supercurrent flows in the x-direction, $\theta = a + bx$.

$$\psi = \cos(a + bx) + i \sin(a + bx)$$

$$\psi = \psi_0 \exp i \delta \mathbf{k} \cdot \mathbf{r}$$

$$\nabla \theta = \delta \mathbf{k}, \quad \mathbf{j} = -(e\hbar/m_e)n_s \delta \mathbf{k}$$





Inside the barrier, the macroscopic wavefunction is

$$\psi(x) = A \exp \alpha x + B \exp -\alpha x \quad \alpha \text{ depends on barrier height; } d = 2a$$

Let θ_1 and θ_2 be the phases on either side of the insulator.

Continuity conditions: $A \exp -\alpha a + B \exp \alpha a = (n_s)^{1/2} \exp i\theta_1$ and
 $A \exp \alpha a + B \exp -\alpha a = (n_s)^{1/2} \exp i\theta_2$

Hence $A = (n_s)^{1/2} \{ \exp i\theta_2 \exp \alpha a - \exp i\theta_1 \exp -\alpha a \} / \{ \exp 2\alpha a - \exp -2\alpha a \}$
 and $B = (n_s)^{1/2} \{ \exp i\theta_1 \exp \alpha a - \exp i\theta_2 \exp -\alpha a \} / \{ \exp 2\alpha a - \exp -2\alpha a \}$

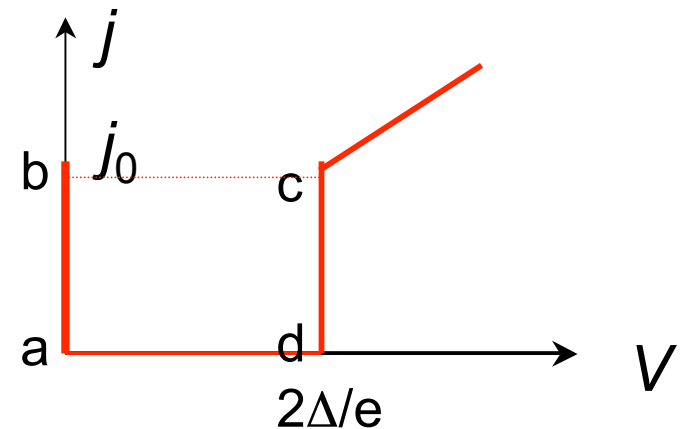
Then $j = (ie\hbar\alpha/m) \{ AB^* - A^*B \} = (4e\hbar\alpha/m)n_s \sin(\theta_1 - \theta_2) / (\exp 2\alpha a - \exp -2\alpha a)$

$j = j_0 \sin(\theta_1 - \theta_2)$

 where $j_0 = (4e\hbar\alpha/m)n_s / (\exp 2\alpha a - \exp -2\alpha a)$

A supercurrent flows across the junction when $V = 0$. It depends on the properties of the insulating barrier, a and α . The barrier *creates* the supercurrent ! j_0 is the maximum possible supercurrent density. It is the critical current of the junction. When $\alpha a \ll 1$, $j_0 = (e\hbar/ma)n_s$. The magnitude of the supercurrent depends on the phase difference $(\theta_1 - \theta_2)$ across the junction.

The junction carries a normal current and a supercurrent, Below j_0 the supercurrent dominates. If the current is increased, when it reaches j_0 the junction switches to the normal state (b - c). On decreasing the current to zero, the device follows c - d, and then returns to a. The Josephson junction is a fast bistable switch. Only the dc current is plotted in the figure. This is the dc Josephson effect.



But when a voltage V is applied across the junction, there is also a rapidly-oscillating ac supercurrent, the ac Josephson effect.

ac Josephson effect.

When a voltage is applied to the junction, electrons may:

- i) tunnel as normal individual electrons when $V \gg 2\Delta/e$
- ii) Tunnel as Cooper pairs. When a pair crosses the junction, it must lose its extra energy to attain the condensed state, which it does by emitting a photon with energy

$$h\nu = 2eV$$

V is typically 1 mV (≈ 10 K) $1 \text{ mV} \rightarrow \nu = 2 \times 1.6 \cdot 10^{-22} / 6.6 \cdot 10^{-34} = 484 \text{ GHz}$, hence ν is in the microwave range.

The junction emits microwaves when a voltage is applied across it.

An ac current tunnel current of this frequency also appears across the junction.

Since frequency can be measured very accurately, the Josephson junction is used in standards laboratories worldwide to define the volt.

When the energy of the centre of mass of the pair is E , a factor $\exp -iEt/\hbar$ must be included in ψ . $\theta = 2eVt/\hbar$ Time varying current $\rightarrow \nabla\theta(t) = 2eV = \hbar d\theta/dt$ implies a voltage. The Josephson junction equation becomes

$$j = j_0 \sin(\theta_1 - \theta_2 - 2eVt/\hbar)$$

The supercurrent is now sinusoidal with $\nu = 2eV/\hbar$, $\omega = 2eV/\hbar$

Finally, if the Josephson junction is irradiated with microwaves of frequency ω' and amplitude V'_0 $V' = V'_0 \sin \omega't$ the equation becomes

$$j = j_0 \sin\{ \theta_1 - \theta_2 - 2eVt/\hbar + (2eV'_0/\hbar) \sin \omega't \}$$

Expand using $\sin(A + B) = \sin A \cos B + \cos A \sin B$
 where $A = \theta_1 - \theta_2 - 2eVt/\hbar$ and $B = (2eV'_0/\hbar) \sin \omega't$

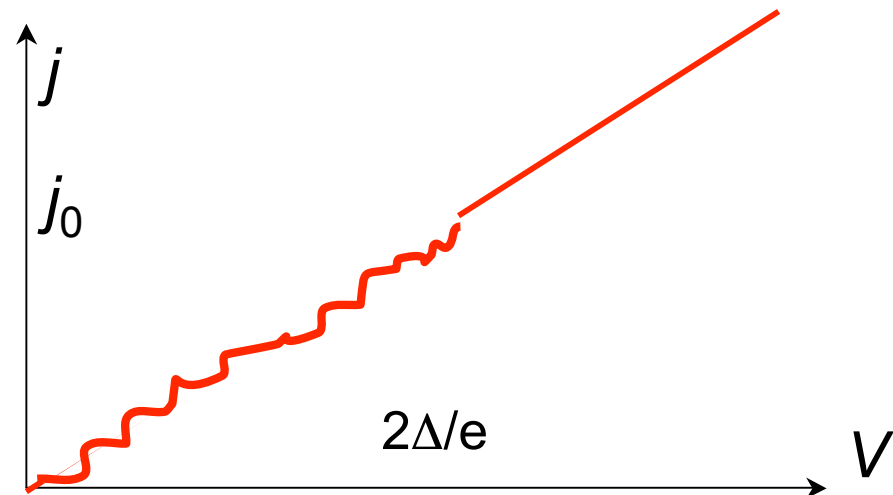
Also expand $\sin(2eV'_0/\hbar) \sin \omega't$ and $\cos(2eV'_0/\hbar) \sin \omega't$ as Fourier series.

$$\rightarrow j = j_0 \sum_0^\infty A_n \sin\{ \theta_1 - \theta_2 - (2eV/\hbar - n\omega')t \}$$

Hence, as V increases, a dc current flows when $V = n \hbar \omega'/2e$

Shapiro steps occur when V is a multiple of $\hbar\omega'/2e$

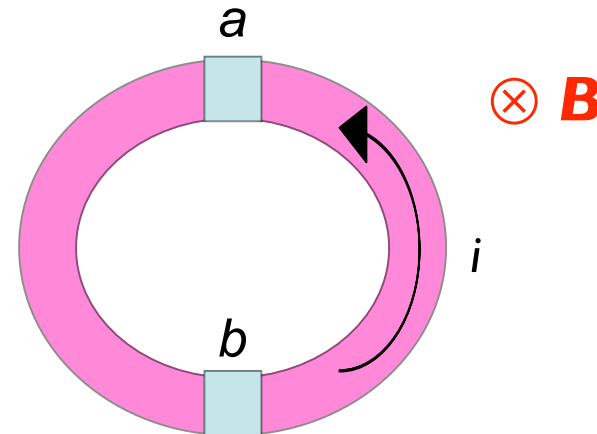
This gives \hbar/e from $V'_0(\omega)$ measurements



dc SQUIDS

Now combine Josephson junctions with the idea of flux quantization in a ring. There must be two junctions in the ring if we are to be able to apply or measure a dc voltage across it.

The junctions may be tunnel junctions, or point contacts (weak links) with a much reduced i_c .



Suppose the two junctions are identical. The phase jumps across the junctions are $\Delta\theta_a$ and $\Delta\theta_b$. These decide the supercurrent flowing in the ring.

When the field is applied, a supercurrent flows in the ring so as to exclude it. However, if $i > i_{ca}$ for the weak links, the flux cannot be entirely excluded from the ring. It penetrates, one fluxon at a time, and the direction of the current in the ring changes sign periodically as B_0 is increased.

[Read](#) Ross-Innes and Rhoderick, Ch II.

If the weak links were absent, the applied field would cause a supercurrent to flow in the loop in order to exclude the flux. The flux penetrates the ring when the critical current density j_c of the superconductor is reached.

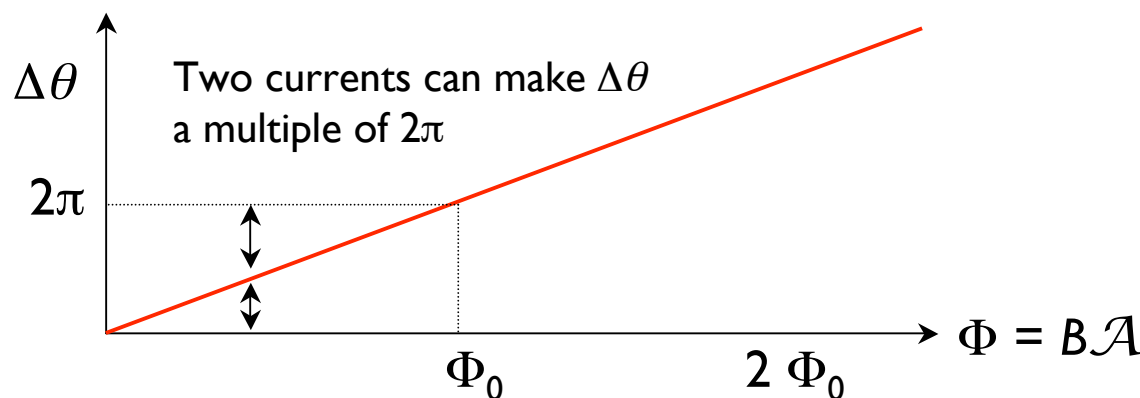
When the weak links are present, the flux penetrates as soon as the critical current density of the junction j_{ca} is reached. It penetrates one fluxon at a time, and the sense of the supercurrent in the ring reverses periodically as B increases. In general $Li_{ca} \ll \Phi$, and in the device we consider $Li_{ca} \ll \Phi_0$ so all flux is penetrating the ring.

From §4.5, we can write the condition for flux quantization around the ring,

$$\oint \mathbf{j} \cdot d\mathbf{l} = (n_s q/m) \oint \{ \hbar \nabla \theta - q \mathbf{A} \} \cdot d\mathbf{l} = 0$$

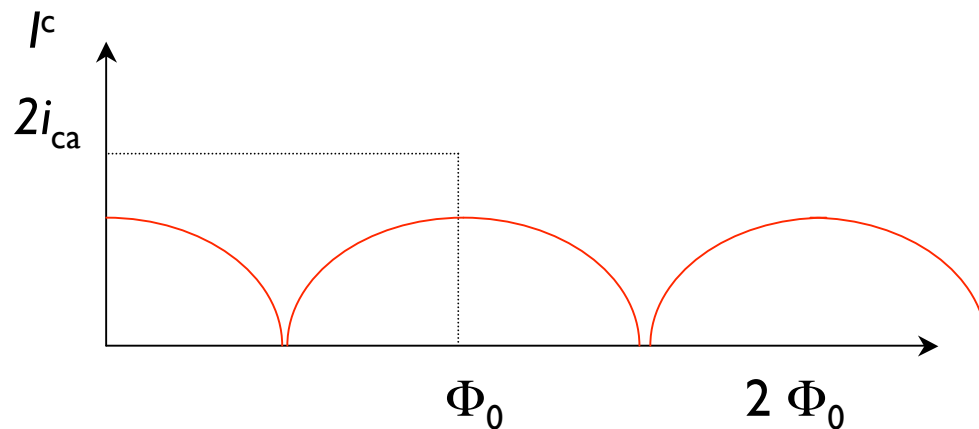
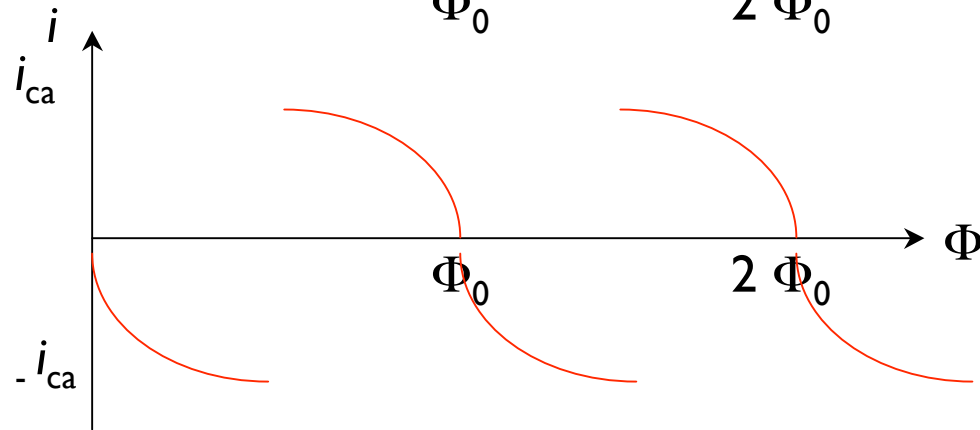
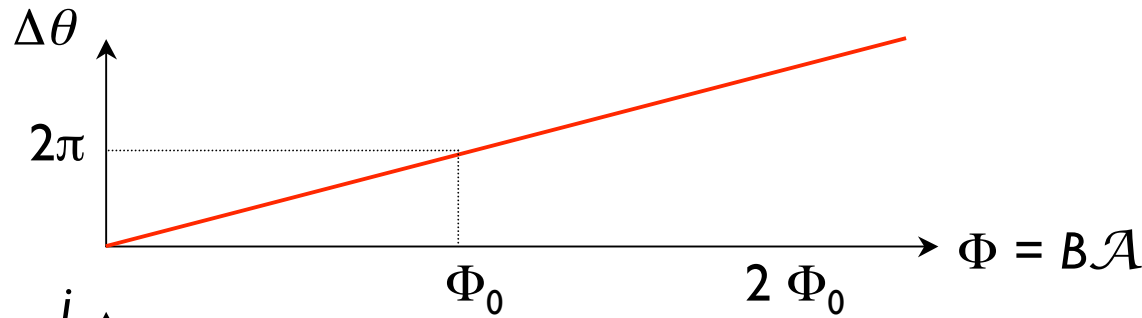
The phase change around the superconducting circuit is $2n\pi$.

$$\hbar [(\Delta\theta_a - \Delta\theta_b) + 2\pi n] - q\Phi = 0 \quad \text{hence } \Delta\theta + 2\pi n = 2\pi\Phi/\Phi_0$$



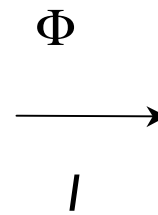
Since $Li_{ca} \ll \Phi_0$ the induced circulating current cannot even generate one fluxon. The flux in the ring $\sim \Phi_a$

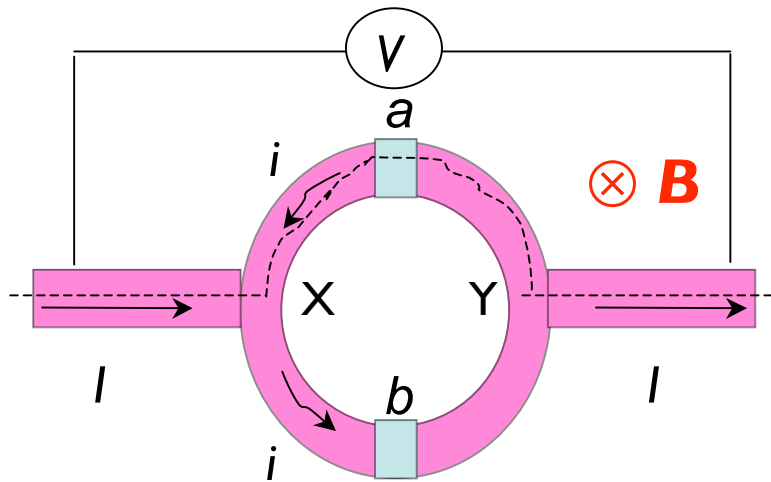
The quantum condition that the phase change around the ring is $2n\pi$ is satisfied because of the phase differences at the weak links. $\Delta\theta(B) = \int (2e/\hbar) \mathbf{A} \cdot d\mathbf{l} = 2\pi\Phi/\Phi_0$



The current in the loop oscillates between i_{ca} and $-i_{ca}$ as the applied field is increased. The loop will contain an integral number of fluxons when it is superconducting.

The current oscillations are detected by means of a sense current I ,





Pass a sense current I across the SQUID. Half of it passes in each arm. There is a current of $I/2 - i$ in junction a , and a current of $I/2 + i$ in junction b .

If θ_0 is the phase difference between X and Y associated with I .

$$\Delta\theta_a = \theta_0 - \pi\Phi/\Phi_0 \quad \Delta\theta_b = \theta_0 + \pi\Phi/\Phi_0$$

$$J_a = j_0 \sin(\theta_0 - \pi\Phi/\Phi_0) \quad J_b = j_0 \sin(\theta_0 + \pi\Phi/\Phi_0)$$

$$J = J_a + J_b = j_0 [\sin(\theta_0 - \pi\Phi/\Phi_0) + \sin(\theta_0 + \pi\Phi/\Phi_0)]$$

$$J = 2j_0 \sin \theta_0 \cos(\pi\Phi/\Phi_0)$$

$$J_c = 2j_0 |\cos(\pi\Phi/\Phi_0)|$$

There is interference between the currents going around the two paths.

SQUIDS are used as very sensitive magnetometers, flux changes of $\Phi_0/100$ can easily be detected.

Suppose the area of the loop is 1 cm^2 , 10^{-4} m^2 .

$$\Phi_0 = 2 \cdot 10^{-15} \text{ T m}^2$$

$$B_{\min} = (1/100) \times 2 \cdot 10^{-15} / 10^{-4} = 2 \cdot 10^{-13} \text{ T} !$$

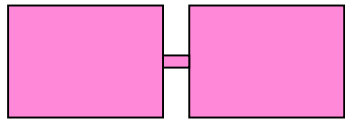
Hence we use SQUIDS to detect the very weak fields produced by the biological currents produced in the heart, brain etc.

Geological prospection. SQUIDS are used to map anomalies in the Earth's magnetic field that reflect buried iron ores.

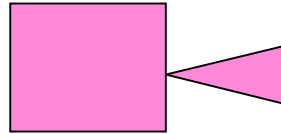
The SQUID is used as a sensitive ammeter to measure very very small currents *via* the fields they produce. Small voltages are measured by passing currents through a known resistor.



There are various types of 'weak links', all of them showing a small critical current across the constriction, where magnetic field can penetrate.



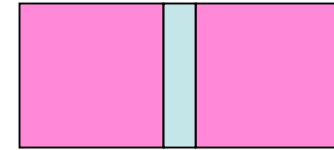
Nanoconstriction



Point contact



Grain boundary



Tunnel junction

A supercurrent can pass through the weak link, and the phase difference $\Delta\theta$ increases with current, reaching the critical value when $\Delta\theta = \pi/2$. Only for the tunnel junction does the current vary as the sine of $\Delta\theta$, but otherwise all the weak links resemble each other.

A short weak link has $d < \xi$. The ideal Josephson effect is seen only in short links

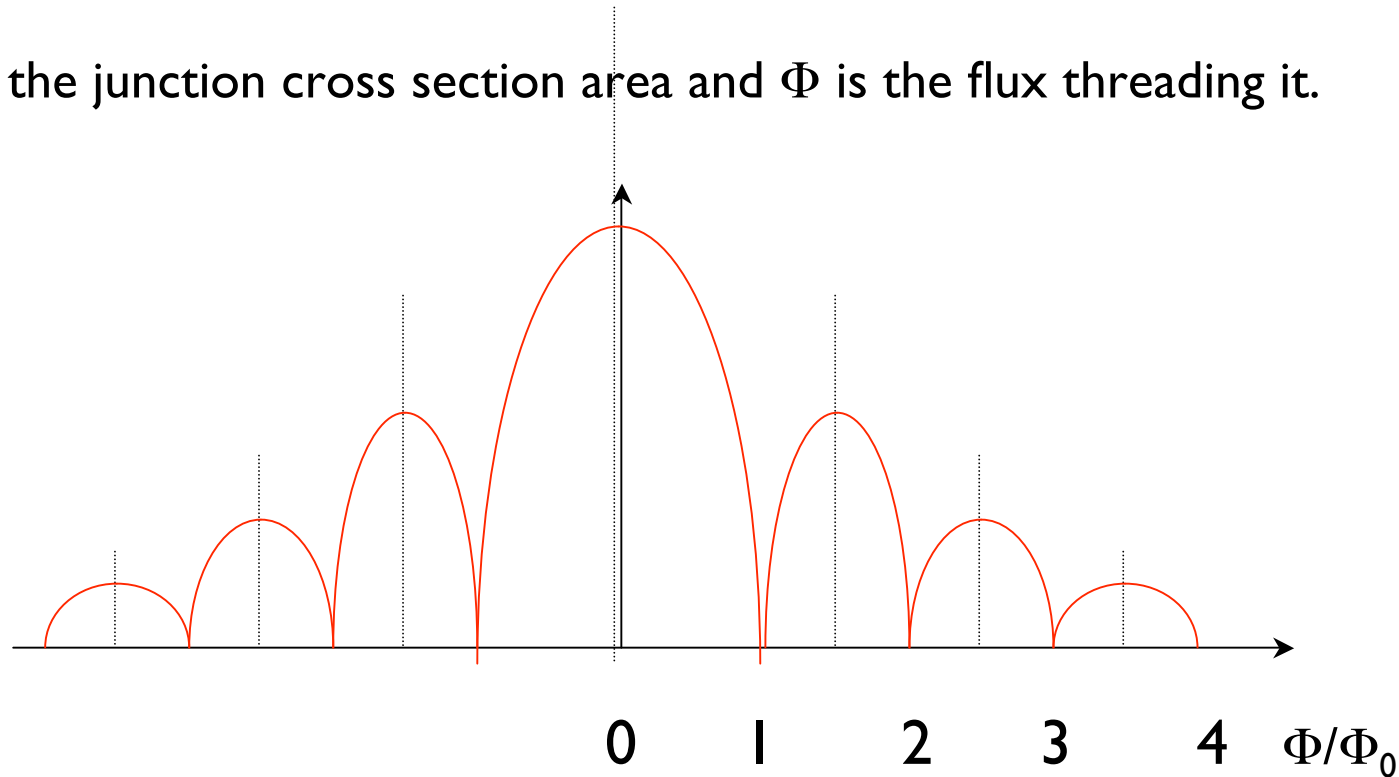
The point contact junctions are most suitable as rf radiation sources and detectors, as the radiation can be easily coupled in and out of them.

A layer of normal metal can also be used to separate the two superconductors.

A single Josephson junction is sensitive to the flux threading it. There is a dc current which depends on the flux threading it.

$$J = j_0 a [\sin(\pi\Phi/\Phi_0) / (\pi\Phi/\Phi_0)] \sin \Delta\theta$$

Here a is the junction cross section area and Φ is the flux threading it.



This resembles the Fraunhofer diffraction pattern from a single slit.

— Switching of a Josephson junction can be very fast; We can estimate the switching time from the junction capacitance C , and the critical current I_0 and the switching voltage $V_{\text{switch}} = 2\Delta_0/e$

$$\tau_{\text{switch}} \approx R_n C = C V_{\text{switch}} / I_0$$

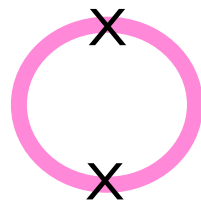
$C = \epsilon\epsilon_0 a/d$ where a is the junction area and $d = 2a \approx 1 \text{ nm}$; $R_n \sim 1/a$

Hence the switching speed is *independent* of area. This means that a scalable technology could be built around superconducting electronics. The switching speed depends on the superconducting material, and the barrier thickness d . (which must be as thin as possible)

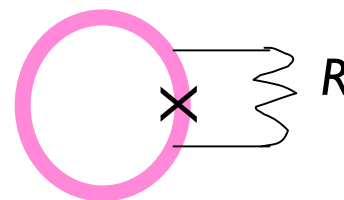
$I_0 = (2\Delta_0/eR_n)$. A $100 \times 100 \mu\text{m}^2$ junction may have $R \approx 0.1 \Omega$ and $C \approx 4 \cdot 10^{-10} \text{ F}$
 For a conventional superconductor $2\Delta_0/e \approx 1 \text{ mV}$, $I_0 \approx 0.1 \text{ mA}$, $j_0 = 10^6 \text{ A m}^{-2}$

$$\tau_{\text{switch}} \approx 4 \cdot 10^{-12} \text{ s}$$

— Suppress the hysteresis of a Josephson junction by placing a resistive shunt across the junction (RSJ)



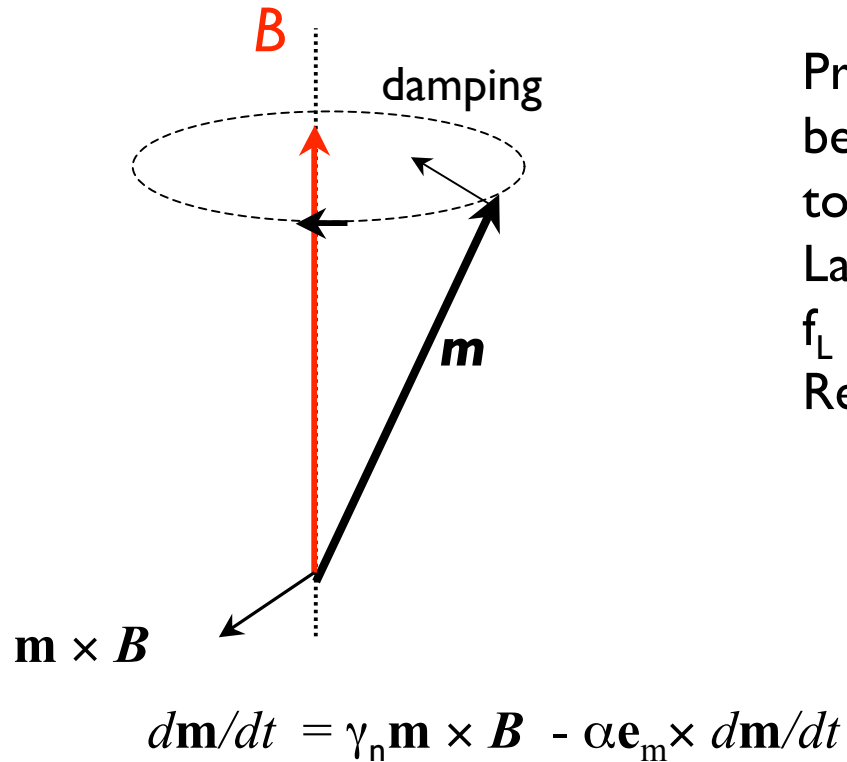
dc SQUID



rf SQUID

4.5 Resonance sensors

4.5.1 Proton resonance magnetometer.

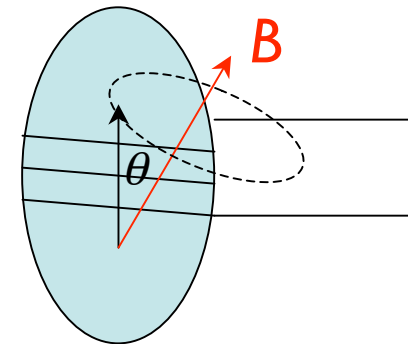


Torque creates precession at the Larmor frequency

$$f_L = \gamma_n B / 2\pi$$

where $\gamma_n = 42.57637 \text{ MHz/T}$

Protons (in water or kerosene for example) can be polarized by a field pulse, and then allowed to precess freely (free induction decay) at the Larmor frequency in the field to be measured. f_L in the Earth's field is $\sim 2 \text{ kHz}$. Relaxation times \sim seconds.



The same coil serves to polarize the protons, and as a pickup for the kHz precession signal.

Note:

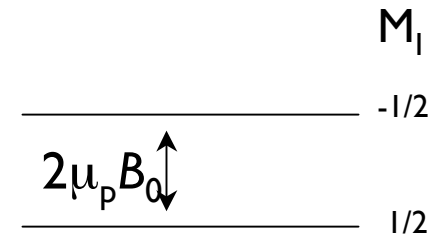
1) The proton has nuclear spin $I = 1/2$. Its angular momentum is $\hbar/2$. The magnetic moment is $\mu_p = 2.793 \mu_N$ where the nuclear magneton, $\mu_N = eh/m_p$ is $5.051 \cdot 10^{-27} \text{ Am}^2$.

2) The moment induced by the applied field B_0 is very small:
 If $B_0 = 0.1 \text{ T}$, then $\mu_p B_0/kT = 1.26 \cdot 10^{-7}$ at RT

$$\langle m \rangle = \mu_p [1 - \exp(-2\mu_p B_0/kT)] / [1 + \exp(-2\mu_p B_0/kT)]$$

$$\langle m \rangle = \mu_p (-\mu_p B_0/kT)$$

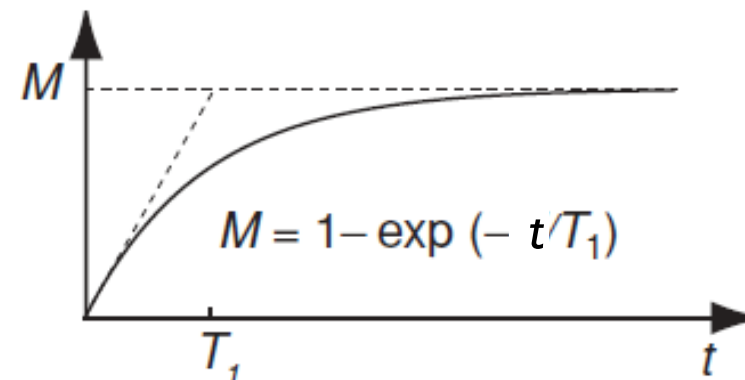
$M_0 = n\langle m \rangle$, where n is the density of protons in water or kerosene



3) The 'spin-lattice' relaxation time T_1 needed to establish equilibrium when B_0 is switched on is \sim seconds.

$$M(t) = M_0(1 - \exp -t/T_1)$$

	T_1 (s)
Distilled water	2 - 3
Deoxygenated water	3.1
Kerosens	0.5



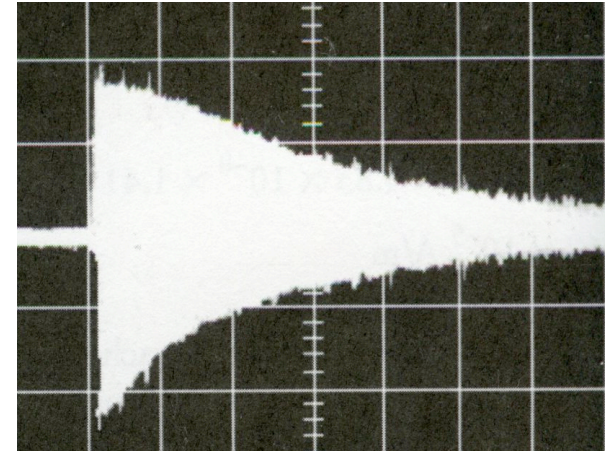
- 4) The spin dephasing or 'spin-spin' relaxation time T_2 for the free induction decay,

$$M(t) = M_0 \exp(-t/T_2),$$

is $T_2 < T_1$.

The digital time sequence is fitted, or Fourier analysed in order to determine f_L as precisely as possible. A precision of 1 Hz corresponds to sensitivity of 24 nT. 1 nT sensitivity is possible

The Earth's field is $\sim 50,000$ nT

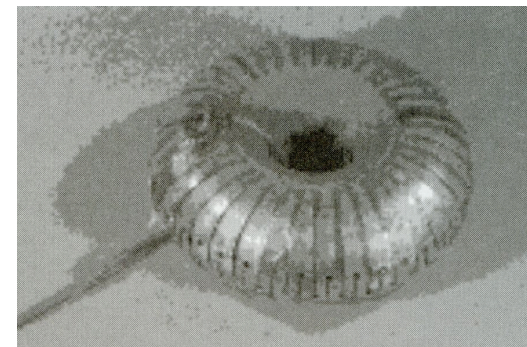


- 5) There is a 'null cone' whose axis is the direction of the field where the sensitivity drops to zero. The Larmor precession frequency is independent of angle, but when $\theta = 0$, there is no change of flux in the coil, so no induced emf.

A solution is to use a toroidal container and coil.

Some parts are always perpendicular to \mathbf{B} .

The signal varies as $(2 - \sin^2 \alpha)$, where α is the angle between \mathbf{B} and the toroid axis

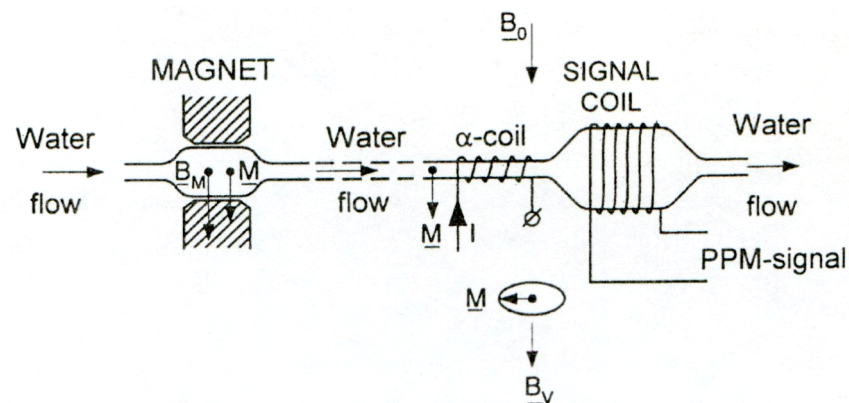


- 6) The demagnetizing field will decay with characteristic time T_2 , causing the larmor frequency f_L to increase slightly with time. The demagnetizing correction to the measured B is

$$\mu_0 H_d = -\mu_0 \mathcal{N} M(t)$$

Here $\mathcal{N} = 1/3$ for the sphere, and 0 for the toroid.

- 7) Signal-noise ration for a proton magnetometer for the Earth's field is ~ 100
- 8) Stronger signals can be achieved in a flow system, with a strong permanent magnet, $B_0 \sim 1$ T.
- 9) The polarizing field must be switched off sufficiently fast so that the magnetization cannot follow the changing field adiabatically.



4.5.2 Overhauser magnetometer.

Electrons have spin $S = 1/2$ and moments of one Bohr magneton $\mu_B = eh/m_e$, about 400 times greater than that of the proton. In an applied field B_0 the induced moment $\langle m \rangle / \mu_B$ is 400 times $\langle m \rangle / \mu_p$.

But usually, the electron spins are paired up in chemical bonds, so they do not respond to the magnetic field.

Free radicals are chemical species with an unpaired electron, and $S = 1/2$. The Larmor precession frequency of the electron is $\approx 28 \text{ GHz T}^{-1}$.

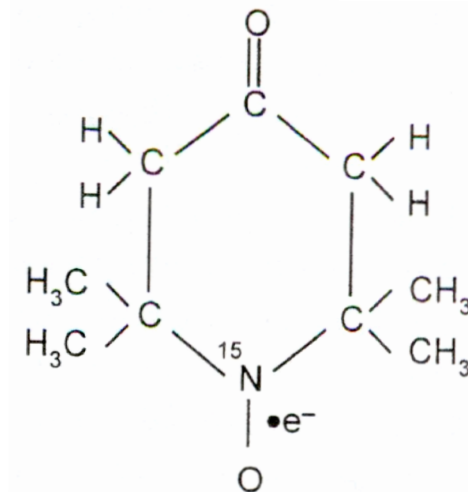
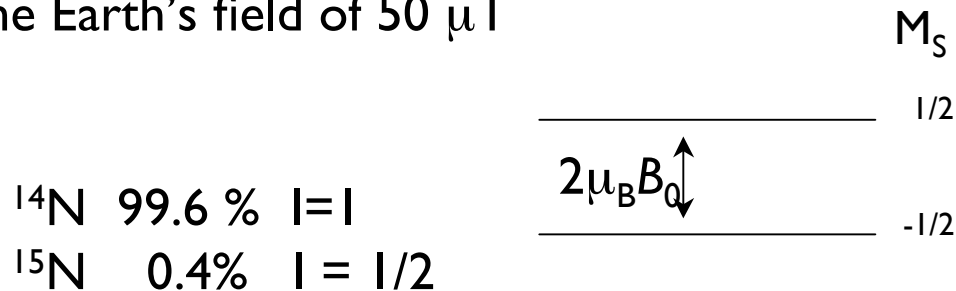
Electrons and nuclei interact by hyperfine interactions. The electrons can create magnetic fields and electric field gradients at the nuclei. These electron - nucleus interactions can transfer polarization across to the nuclei, the *Overhauser effect*.

In the case of protons (hydrogen) in water or kerosene, apply the field B_0

Polarize the electrons \rightarrow Hyperfine interaction \rightarrow Strongly polarize the protons

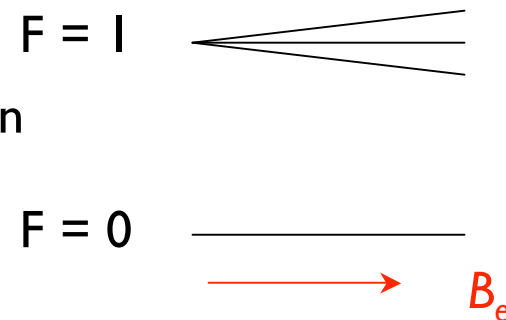
Since the electron spins of the hydrogen atoms are paired, we need to add some free radical. Ideal is Tempone, which is diluted in the water or kerosene. It is stable, and not particularly aggressive.

Normally, for electrons, the resonance frequency of 28 GHz/T corresponds to a peak at about 1.5 MHz in the Earth's field of 50 μ T



Hyperfine interaction of the electron with the ^{15}N nucleus produces a zero-field splitting of 60 MHz. Hyperfine field is 2.1 mT. The liquid is polarized in a 60 MHz resonant cavity.

When the spin polarization has been transferred to the protons, a short 90° pulse turns the proton spins perpendicular to the Earth's field, which is measured by the free-induction decay, as before.



An alternative free radical is trityl, which has no hyperfine interaction, and no zero field splitting.

The esr linewidth is only $2.5\mu\text{T}$. Since the saturation power $\sim \Delta B^2$, the power for saturation is much reduced

For a 7 ml volume, a signal/noise ratio of $55 \text{ dB/Hz}^{1/2}$ for 50,000 nT, with a power of just 700 mW

Useful for a low-field deep space measurement.

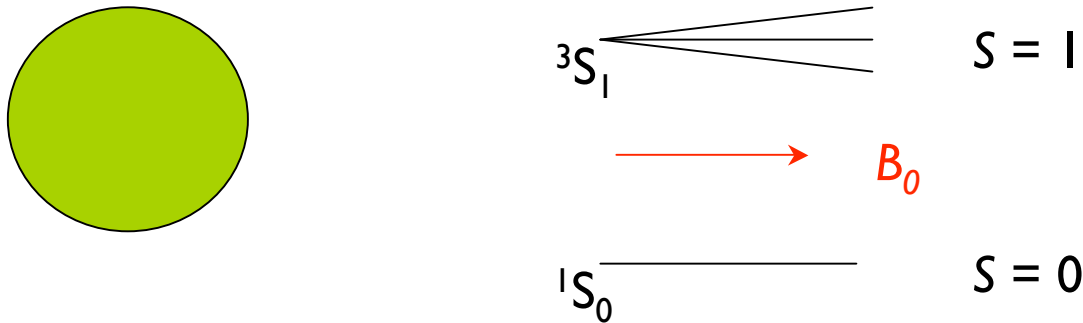
4.5.3 Helium magnetometers.

Helium-3

^3He is a decay product of tritium ^3H .

It has a nucleus with $I = 1/2$, and an abundance of 0.0001 %

The atom is normally in a $1s^2$ spin singlet 1S_0 ground state, but it can be excited to a $1s^12s^1$ spin triplet 3S_1 excited state in a continuous high-frequency glow discharge.



The atom can be spin polarized by an external field, and the polarization transferred to the nucleus by the Overhauser effect.

Notation:

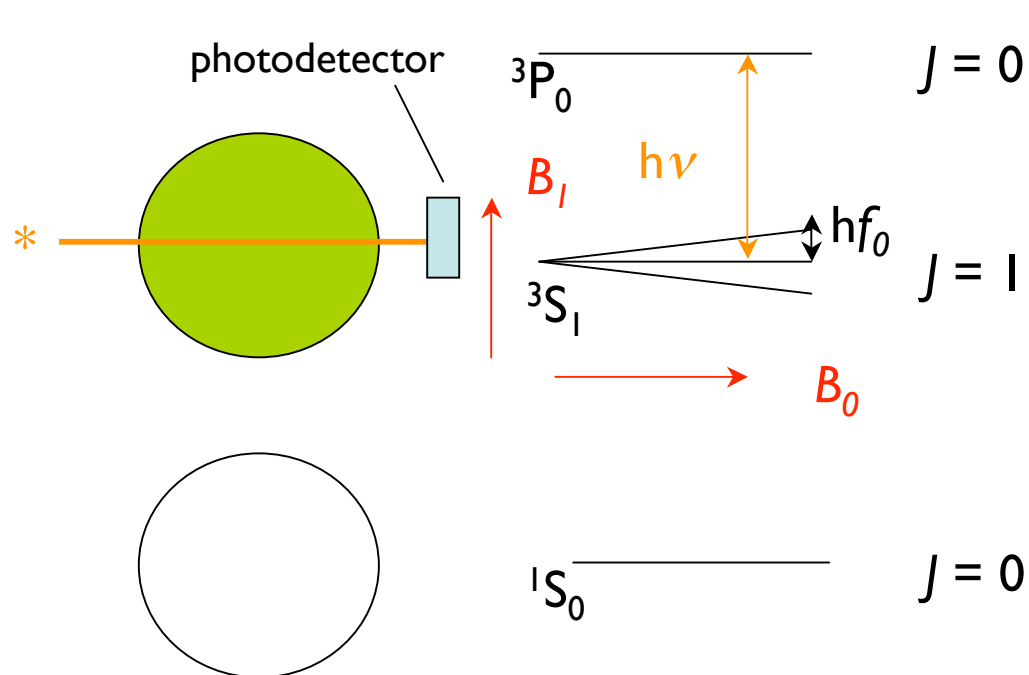
$$2S+1 L_J$$

$$J = L + S$$

4.5.3 Helium magnetometers. Helium-4

The ^4He magnetometer is a ' M_z ' magnetometer that depends only on optical transitions, not nuclear precession.

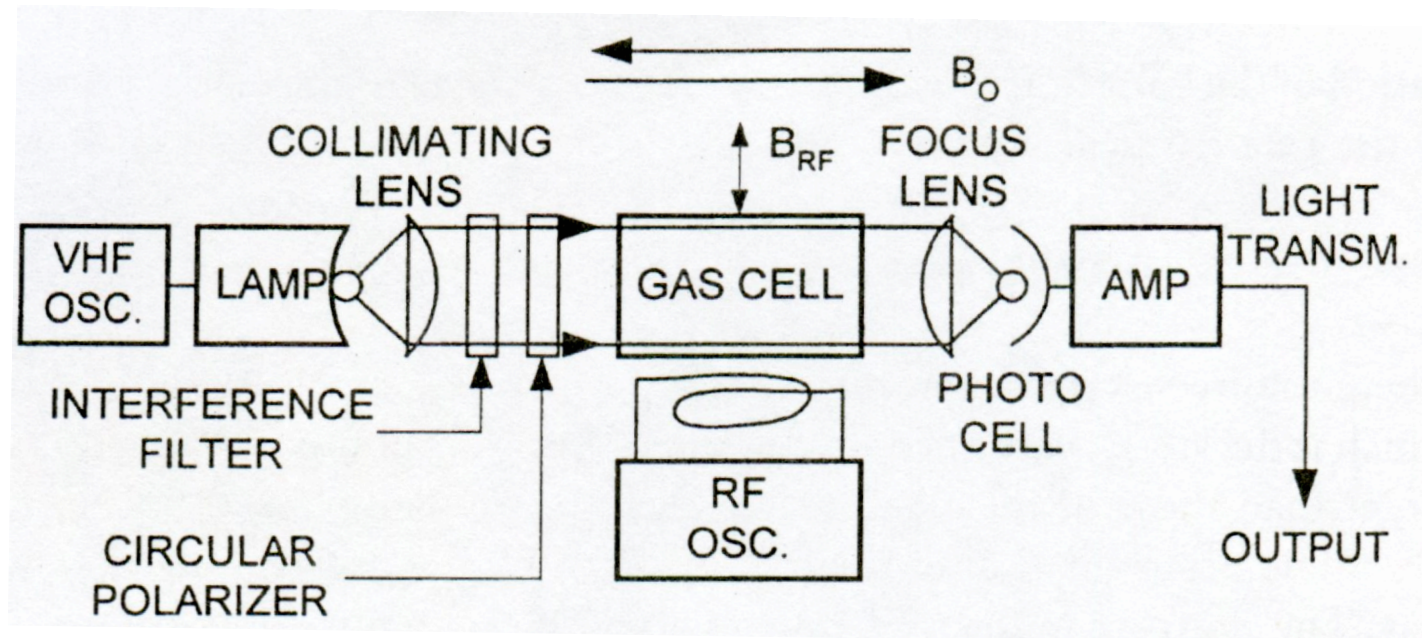
Again a glow discharge is set up, where the gas is excited to a paramagnetic 3S_1 state. Transitions between the levels are induced by a field applied perpendicular to \mathbf{B}_e at a frequency f_0 where $hf_0 = 2\mu_B B_0$. $B(t) = B_1 \cos ft$



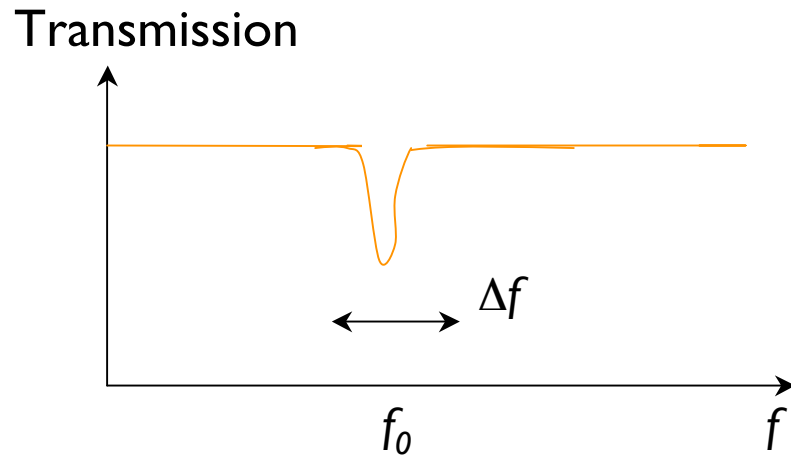
The electrons in the $1s^1 2s^1$ configuration can be excited to $1s^1 2p^1$, 3P_0 configuration. The separation is $h\nu$, where $\lambda = c/\nu = 1083 \text{ nm}$ (infra red).

The atoms are pumped out of the 3S_1 ; $M_j = 0$ level to the 3P_0 ; $M_j = 0$ by unpolarized infra-red light, until the cell becomes transparent to the IR.

The radio frequency f is swept and the resonance is observed. 32



An M_z magnetometer



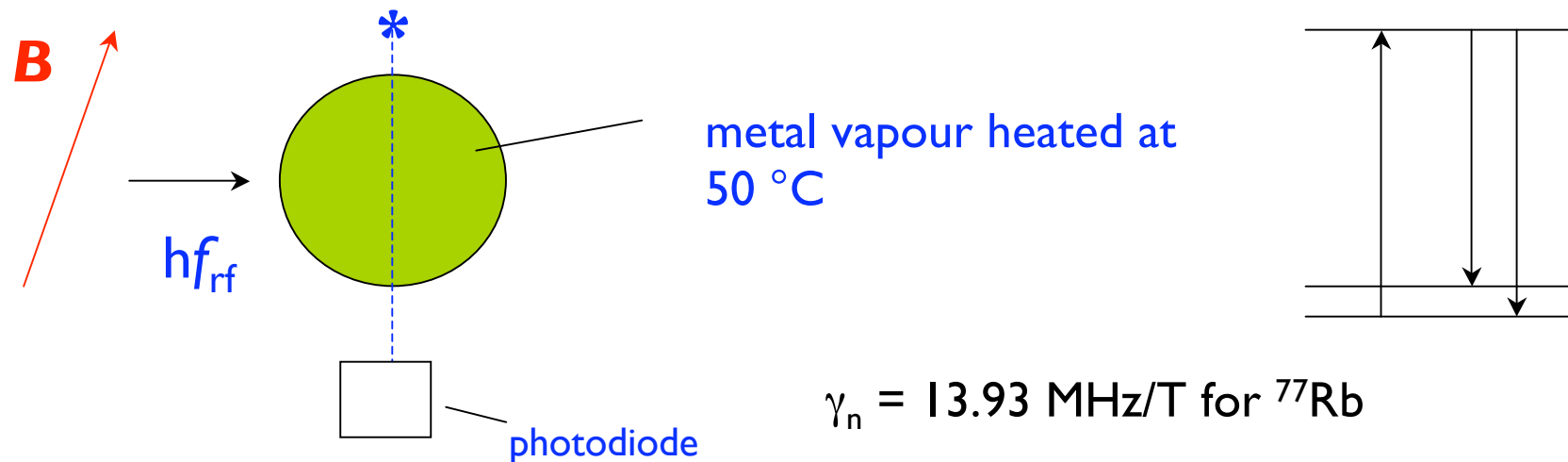
The transparency signal shows a dip at resonance, when the $M_j = 0$ line is repopulated.

Note:

- 1) The D_0 line from $^3S_1 ; M_j = 0$ to $^3P_0 ; M_j = 0$ is independent of field B_0
- 2) The D_1 and D_2 lines from $^3S_1 ; M_j = \pm 1$ to $^3P_0 ; M_j = 0$ depend on field B_0
- 3) If the frequency of rf oscillator is modulated at a low frequency Ω (~ 200 Hz), with swing Δf . The amplitude and phase of the Ω signal from the photocell gives the deviation of the centre frequency from f_0 . There is then a large 2Ω signal. The low frequency centre frequency gives f_0 .
- 4) Two sensors at right angles can be used to eliminate the null cone. It is only the component of \mathbf{B}_1 perpendicular to \mathbf{B}_0 that is effective.

4.5.4 Alkalai vapour magnetometers.

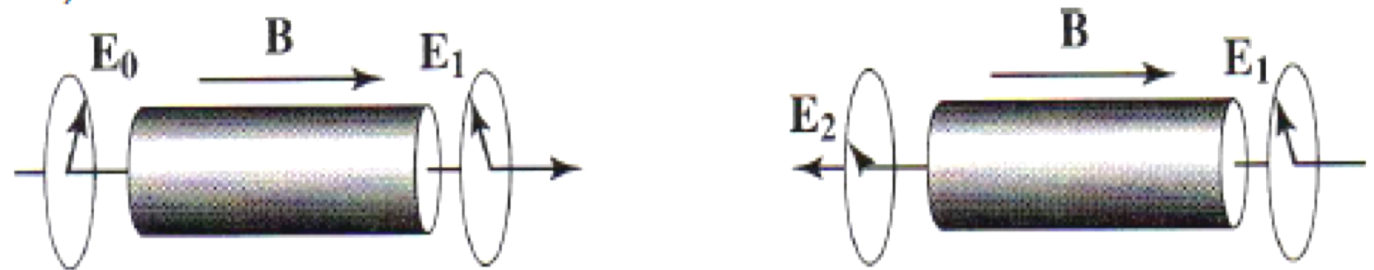
Rb or Cs vapor can be magnetized by optical pumping with circularly-polarized light. When the vapour is fully-polarized, the cell becomes transparent. An rf field is applied to depolarize the vapour, and the optical transparency signal is then modulated at the the nuclear Larmor precession frequency in the applied field. The magnetometer provides an extremely precise, absolute value of the magnitude of the field. These magnetometers have been packaged on a chip.



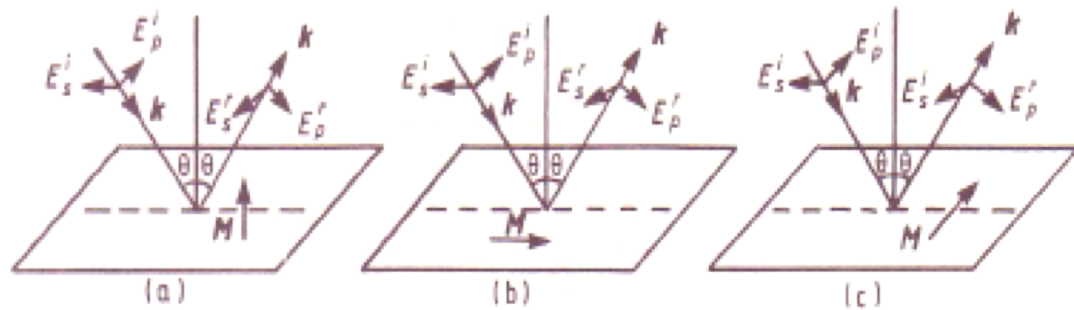
Magnetometer	Sensitivity (nT)	Resolution (nT)	Noise
Proton	0.1	0.01	
Overhauser	0.02	0.01	
^3He			
^4He			
Potassium	0.001		
Rubidium			
Caesium			

4.6 Magneto-optic sensors.

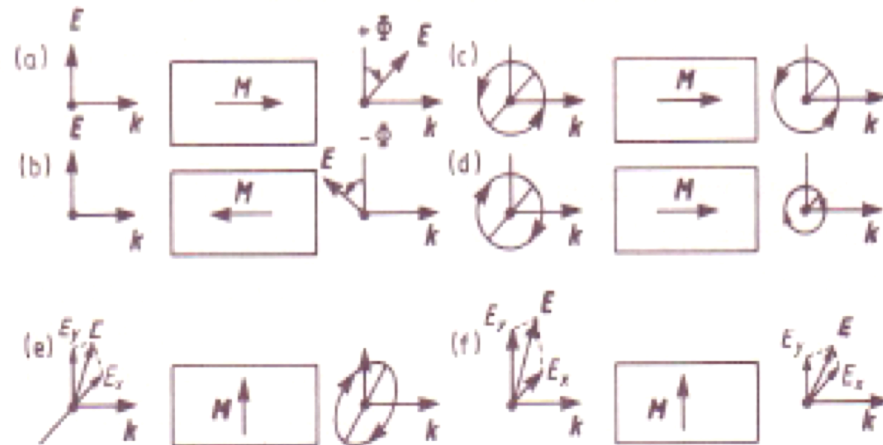
Faraday effect: (transmission)

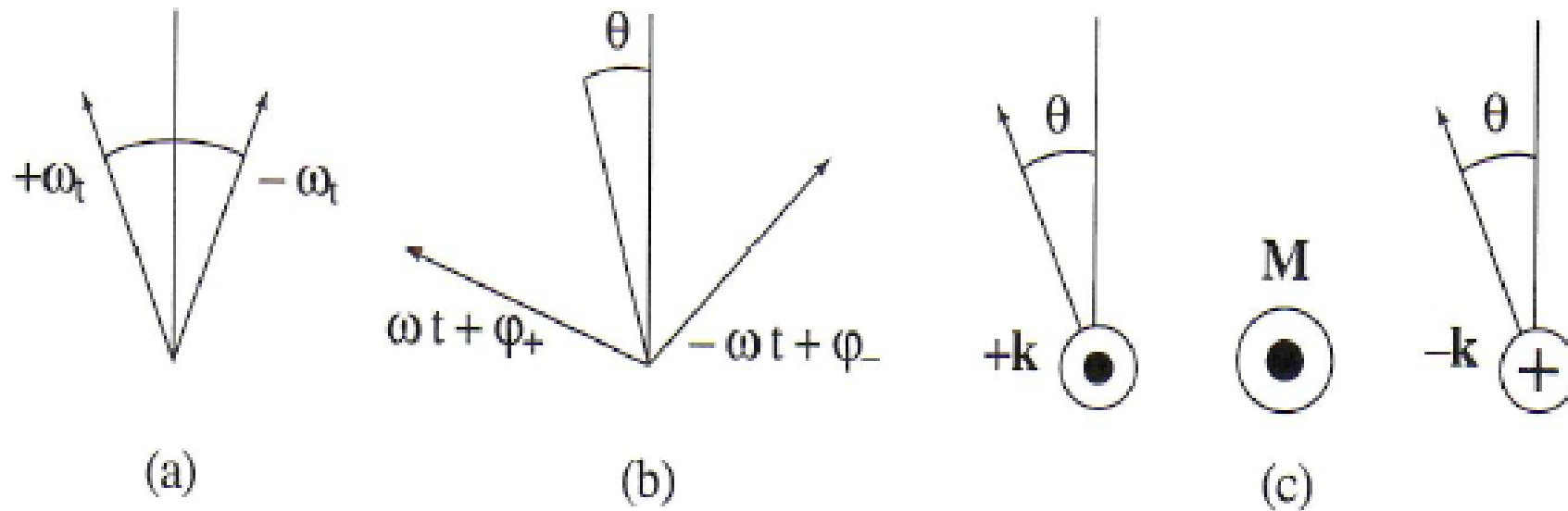


Kerr effect: (reflection)



Dichroism and birefringence





A plane-polarised wave is decomposed into the sum of two, counter-rotating circularly-polarized waves (a) which become dephased because they propagate at different velocities (b) through the magnetized solid. The Faraday rotation θ is non-reciprocal - independent of direction of propagation.

The Faraday rotation θ_F is the rotation of the plane of polarization as passes through a transparent medium. The constant of proportionality depends on the Verdet constant k_V .

$$\theta_F = k_V \int \mu_0 \mathbf{M} \cdot d\mathbf{l}$$

θ_F is conventionally positive when rotation is clockwise when facing the source.

e.g. for water the rotation is 3.9 radians $T^{-1}m^{-1}$. It is $\sim 10^5$ times greater for transparent ferromagnets or ferrimagnets.

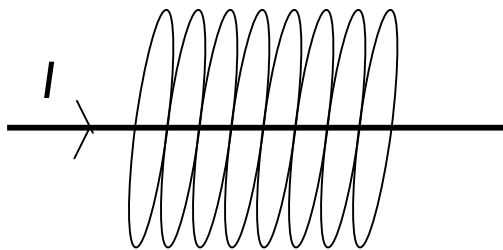
Optical fibre field sensors, based on magneto-optic Faraday effect.
They are bulky, and used for large fields.
Long coils of optical fibres can be used as optical current sensors.

Since, by Ampere's law $I = \oint \mathbf{H} \cdot d\mathbf{l}$

$$\text{and } \mathbf{M} = \chi \mathbf{H}$$

$$\mu_0 I \chi = \oint \mu_0 \mathbf{M} \cdot d\mathbf{l}$$

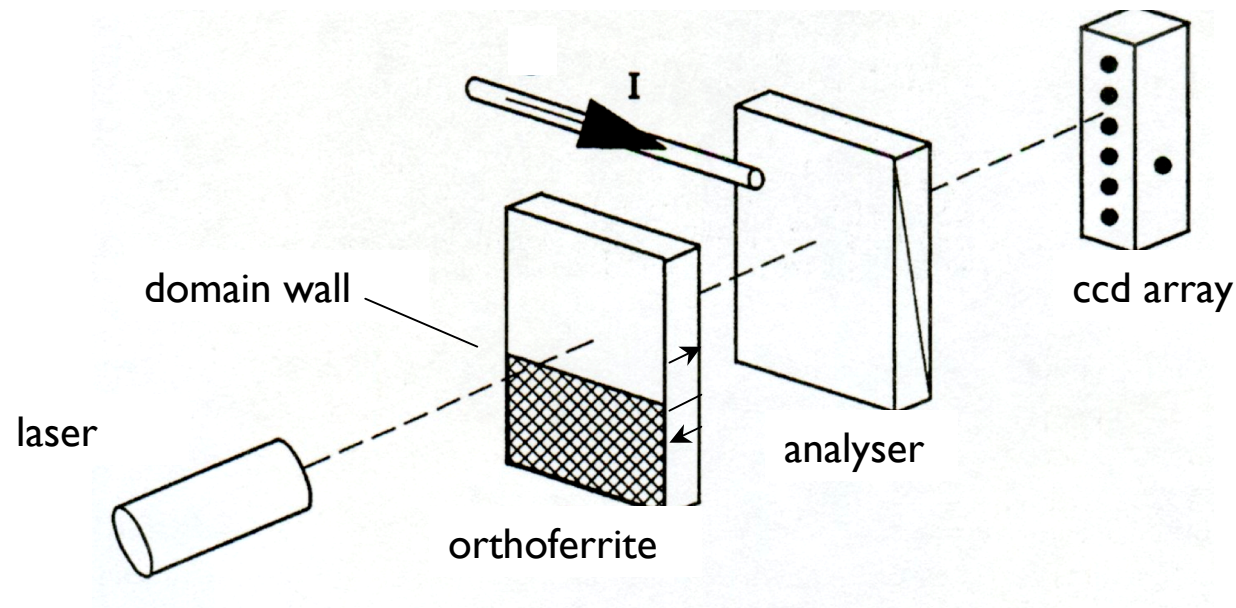
$$I = \theta_F / nk_V \mu_0 \chi$$



Domain wall current sensor

The Faraday effect is also observed in transparent ferromagnets. Since the Faraday rotation depends on $\int \mu_0 \mathbf{M} \cdot d\mathbf{l}$, a much shorter path length is needed - tens of microns instead of meters.

Material	Formula	T_c (K)	Spin structure	$\mu_0 M_s$
YIG	$Y_3Fe_5O_{12}$	560	Ferrimagnet	0.18
Yttrium Orthoferrite	$YFeO_3$	xx	Canted antiferromagnet	



$\text{Y}_3\text{Fe}_5\text{O}_{12}$; YIG

Garnet;

$a_0 = 1238 \text{ pm}$,

A synthetic garnet, with iron in tetrahedral [24d] and octahedral {16a} sites. The Y and O form a \approx close-packed array.



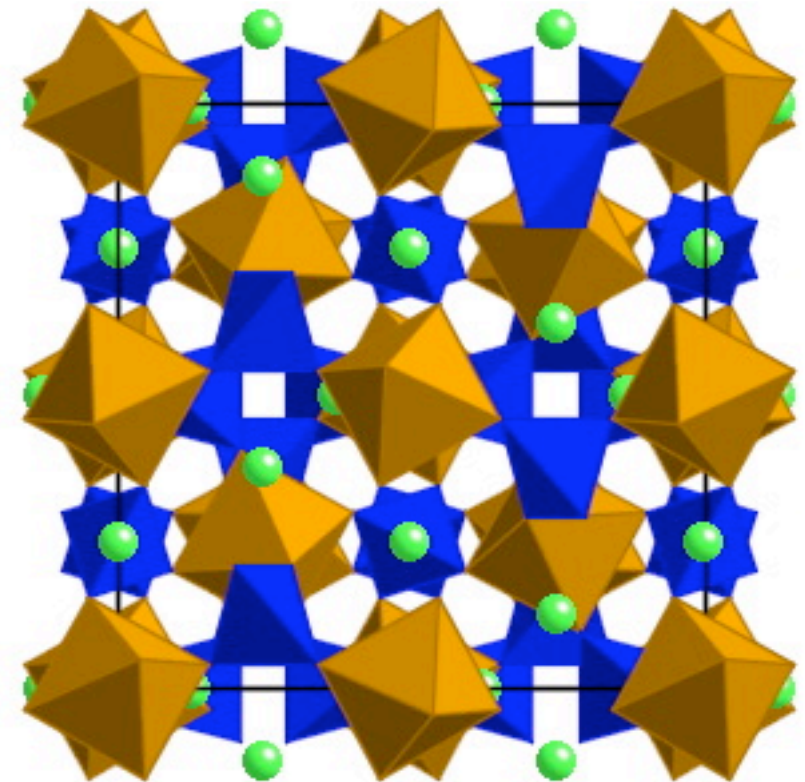
YIG – Yttrium Iron Garnet is a green ferrimagnetic insulator.

The magnetic structure is $24d\uparrow, 16a\downarrow$

$T_C = 560 \text{ K}$ $\mu_0 M_s = 0.18 \text{ T}$ $m_0 = 5.0 \mu_B/\text{fu}$

YIG is an insulator with excellent high-frequency magnetic properties., and a very narrow ferromagnetic resonance linewidth. It is used for microwave components.

Also useful as a magneto-optic material, especially when doped with Bi.





Yttrium orthoferrite; $a \approx 0.58$ nm

A tetragonally-distorted perovskite.

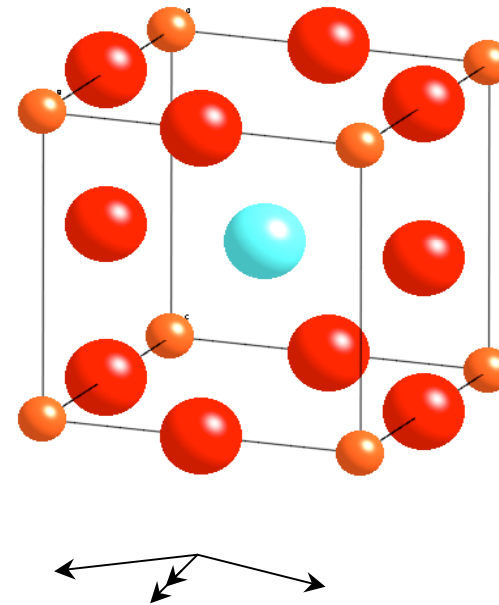
The compound is basically antiferromagnetic due to Heisenberg superexchange

$-J \mathbf{S}_i \cdot \mathbf{S}_j$
(Fe³⁺ - O²⁻ - Fe³⁺ bond), with moments $\perp c$

There is spin canting in the plane due to the feeble Dzialashinsky-Moria coupling

$$-\mathcal{D} \cdot \mathbf{S}_i \times \mathbf{S}_j$$

$$J_s \approx 0.001 \text{ T} \quad T_C = 620 \text{ K}$$



Magneto optic tensor for isotropic material in a magnetic field:

ϵ_{xx}	$-\epsilon_{xy}$	0
ϵ_{xy}	ϵ_{xx}	0
0	0	ϵ_{zz}

ϵ_{xy} is the dielectric constant